



Controlling subcellular localization to alter function: Sending oncogenic *Bcr–Abl* to the nucleus causes apoptosis

Andrew S. Dixon, Mudit Kakar, Korbinian M.H. Schneider, Jonathan E. Constance, Blake C. Paullin, Carol S. Lim *

Department of Pharmaceutics and Pharmaceutical Chemistry, University of Utah, Salt Lake City, UT 84108, United States

ARTICLE INFO

Article history:

Received 16 February 2009

Accepted 23 June 2009

Available online 1 July 2009

Keywords:

Bcr–Abl

Apoptosis

Nuclear localization

Protein switch

CML

ABSTRACT

Altering the subcellular localization of signal transducing proteins is a novel approach for therapeutic intervention. Mislocalization of tumor suppressors, oncogenes, or factors involved in apoptosis results in aberrant functioning of these proteins, leading to disease. In the case of chronic myelogenous leukemia (CML), cytoplasmic *Bcr–Abl* causes oncogenesis/proliferation. On the other hand, nuclear entrapment of endogenous *Bcr–Abl* (in K562 human leukemia cells) causes apoptosis. The goal of this study was to determine whether ectopically expressed *Bcr–Abl* could cause apoptosis of K562 cells when specifically directed to the nucleus via strong nuclear localization signals (NLSs). A single NLS from SV40 large T-antigen or four NLSs were subcloned to *Bcr–Abl* (1NLS-*Bcr–Abl* or 4NLS-*Bcr–Abl*). When transfected into K562 cells, only 4NLS-*Bcr–Abl* translocated to the nucleus. *Bcr–Abl* alone was found to localize in the cell cytoplasm, colocalizing with actin due to its actin binding domain. 1NLS-*Bcr–Abl* also localized with actin. Apoptosis induced by 4NLS-*Bcr–Abl* was evaluated 24 h post-transfection by morphologic determination, DNA staining, and caspase-3 assay. This is the first demonstration that altering the location of ectopically expressed *Bcr–Abl* can kill leukemia cells. Multiple NLSs are required to overcome *Bcr–Abl* binding to actin, thus driving it into the nucleus and causing apoptosis.

© 2009 Elsevier B.V. All rights reserved.

1. Introduction

The causative agent for 95% of all CML cases, *Bcr–Abl*, is derived from the fusion of the breakpoint cluster region (*Bcr*) gene on chromosome 22 and the Abelson leukemia oncogene (*Abl*) on chromosome 9. This reciprocal translocation results in an abnormal, shortened chromosome – ‘Philadelphia chromosome’ or Ph (+) phenotype [1,2]. The resulting *Bcr–Abl* fusion protein acts as an oncoprotein, and the constitutive activation of tyrosine kinase activity of *Abl* leads to cell proliferation. Although Gleevec is currently the ‘gold standard’ drug of choice for *Bcr–Abl* positive CML [3–5], resistance to treatment with Gleevec occurs. This is mostly due to mutations in the *Bcr–Abl* kinase domain that render it unable to bind to Gleevec [6–8]. Some mutations create a more potent *Bcr–Abl* oncogene and accelerate disease progression [9]. Other mechanisms for resistance include *Bcr–Abl* amplification or overexpression, clonal evolution, a decrease in Gleevec bioavailability or cell exposure, and upregulation of drug efflux pumps [6,10]. Many other tyrosine kinase inhibitors (TKIs) are being studied and developed, with a few already approved. Nonetheless, *Bcr–Abl* also has the potential to develop

resistance to these molecules. In addition, since FDA approval, potentially fatal side effects of Gleevec have been uncovered. These include cardiotoxicity [11], the possibility of developing other cancers (due to blockade of tumor suppressor p63) [12], and acute renal failure [13]. Therefore, finding alternative strategies to Gleevec therapy are necessary.

In the cytoplasm *Bcr–Abl* acts as an oncogene by interacting with multiple signal transduction pathways that transmit anti-apoptotic and mitogenic signals [14]. The key pathways involve ras, MAP kinases, the STAT family, PI3 kinase, and myc, among others [15]. In the nucleus, *Bcr–Abl* may cause apoptosis due to nuclear *Abl*'s ability to stabilize p73 and activate its pro-apoptotic functions. Vigneri and Wang have previously shown that nuclear entrapment of *Bcr–Abl* in K562 cells results in apoptosis, and requires an active tyrosine kinase domain to do so [2]. They used Gleevec to stimulate *Bcr–Abl* to go to the nucleus (by unknown mechanism), followed by nuclear entrapment by leptomycin B (LMB), a general inhibitor of nuclear export. After washout of Gleevec, *Bcr–Abl*'s tyrosine kinase activity is re-activated, and the cells undergo spontaneous apoptosis. Unfortunately LMB causes neuronal toxicity and cannot be used therapeutically. This study attempts to address a fundamental question that remains: Does the apoptosis caused by nuclear entrapment of *Bcr–Abl* require depletion of *Bcr–Abl* from the cytoplasm, or is it sufficient to send ectopically expressed *Bcr–Abl* to the nucleus to cause apoptosis?

* Corresponding author.

E-mail address: carol.lim@pharm.utah.edu (C.S. Lim).

2. Materials and methods

2.1. Subcloning and construction of plasmids

Full length *Bcr-Abl* was removed from pEYK3.1 retroviral vector (a kind gift from Dr. George Daley, Harvard Medical School, Boston) using *EcoRI* and cloned into pEGFP-C1 (Clontech, Mountainview, CA) at the *EcoRI* site to make EGFP-*Bcr-Abl*.

The oligonucleotides 5'-CCGGAAGCCCAAGAAGAAGAGAAAAGTGAAT-3' and 5'-CCGGATTCTACTTTCTCTCTTGGGCTT-3' were ligated to pEGFP-*Bcr-Abl* at the *BspEI* site. The oligonucleotide insert encodes for the nuclear localization signal (NLS) from SV40 large T-antigen (amino acids PKKKRKV) and is flanked with the *BspEI* digested sequence. The ligation resulted in the formation of pEGFP-1NLS-*Bcr-Abl* and pEGFP-4NLS-*Bcr-Abl* (a concatemer consisting of four nuclear localization signals).

The bases encoding key residues (T65A and Y66A) in the EGFP chromophore [16,17] of pEGFP-4NLS-*Bcr-Abl* were mutated using the QuikChange II Site-Directed Mutagenesis Kit from Stratagene (La Jolla, CA) to eliminate EGFP fluorescence (for use in some co-transfection experiments). The primers used for the mutagenesis were 5'-CTCGTGACCACCTGCGCGCGGCGTGAGTCTTC-3' and its reverse complement. This plasmid encodes 4NLS-*Bcr-Abl* with non-fluorescent EGFP.

2.2. Cell line and culture conditions

Bcr-Abl positive K562 cells (human chronic myelogenous leukemia cell line), from our collaborator Dr. K. Elenitoba-Johnson (Univ. of Michigan), were cultured as suspension cells in RPMI 1640 supplemented with 10% FBS (Hyclone Laboratories, Logan, UT), 1% penicillin-streptomycin (100U/ml, GIBCO BRL, Grand Island, NY), 0.1% gentamycin (Hyclone), and 1% L-glutamine (Hyclone). Cells were maintained in a 5% CO₂ incubator at 37 °C. Cells were split at a density of 0.5×10^5 /ml two days before transfection.

2.3. Transfection

Transient transfections were performed using Amaxa Nucleofector II according to the Amaxa protocol for K562 cells. Briefly, 2×10^6 cells were pelleted from a cell density of $1\text{--}5 \times 10^5$ cells/mL, and then resuspended in 100 μ L Amaxa Solution V. This solution was then added to 10 μ g DNA and transfected in an Amaxa cuvette using program T-013. Following, 500 μ L RPMI was added to the cuvette and cells were transferred to 15 mL RPMI and plated in a 75 cm² flask for caspase-3 assays. Small aliquots (200 μ L) of cells were plated into 4-well live-cell chambers for fluorescent microscopy (Lab-tek chamber slide system, 2 mL, Nalge NUNC International, Naperville, IL) for determination of transfection efficiency. For co-localization experiments where 2 plasmids were transfected simultaneously, 5 μ g of each plasmid was used; 5 μ g of a single plasmid was used for comparison studies. Cells were incubated for ~20–24 h before any other assays were performed.

To calculate the transfection efficiency, four or more fields of cells were counted under the 40 \times objective. The number of transfected cells (as indicated by the EGFP expression; see methods below for microscope settings) was divided by the total number of cells to obtain transfection efficiency.

2.4. Caspase-3 activity assay

The induction of apoptosis was monitored through the enzymatic activity of caspase-3 using the EnzChek Caspase-3 Assay Kit #1 (Molecular Probes, Eugene, OR) following the manufacturer's protocol. Briefly, 1.5×10^6 cells were pelleted and resuspended in 50 μ L $1 \times$ cell lysis buffer followed by a freeze-thaw cycle. The lysed cells were centrifuged for 5 min at 2100 \times g. As a control, 1 μ L of 1 mM caspase-3 inhibitor was added to one of the lysates of untransfected K562 cells. $2 \times$ substrate

(50 μ L) solution was then added to 50 μ L of lysate and incubated at room temperature for 30 min. A standard curve was made using known amounts of 7-amino-4-methylcoumarin (AMC). Fluorescence was then measured at an excitation wavelength of 355 nm and an emission wavelength of 460 nm. Caspase assays were performed three or more separate times ($n = 3$). Data was represented as relative fluorescence units per cell, taking transfection efficiencies into account (Fig. 5).

2.5. Actin staining and microscopy

K562 cells transfected with EGFP-*Bcr-Abl* were fixed with formaldehyde and stained for actin using BODIPY 558/568 Phalloidin from Molecular Probes (Eugene, OR) according to manufacturer's protocol. Briefly, cells were washed with PBS, pelleted, and resuspended in 4% formaldehyde (in PBS). Cells were incubated in formaldehyde solution for 10 min at room temperature and subsequently washed in PBS. Cells were then placed in 1 mL of 0.1% Triton X-100 (in PBS) for 5 min followed again by washing with PBS. The cells were then incubated with staining solution for 20 min at room temperature and then washed with PBS. Following staining the cells were viewed at 40 \times with an Olympus IX701F inverted fluorescence microscope (Scientific Instrument Company, Aurora, CO) using the HQ:TRITC filter to detect actin, and a high-quantity narrow band GFP filter (excitation HQ480/20 nm, emission HQ510/20 nm, with beam splitter Q4951p) to detect EGFP. Cells were photographed using a F-View Monochrome CCD camera.

2.6. DNA staining and EGFP microscopy

K562 cell nuclei were stained by the addition of 0.8 μ L Hoechst 33342 (10 mg/ml) (Invitrogen, Carlsbad, CA) to 1 mL of cells in a Lab-Tek®II 4-well live-cell chamber (Nalge NUNC) and incubated for 30 min at 37 °C. Pictures were taken approximately 24 h after transfection using a fluorescence microscope with high-quantity narrow band GFP filter (to detect EGFP) and Cyan GFP v2 filter (excitation D436/20 nm, emission D480/40 nm, with beam splitter 455dclp) to detect H33342. To minimize photobleaching of EGFP chromophore, cells were imaged using neutral density filters in combination with short exposure times. An air stream incubator (Nevtek ASI 400, Burnsville, VA) with a variable temperature control was used to maintain the microscope stage and the live-cell chambers at 37 °C. All filters were purchased from Chroma Technology (Brattleboro, VT).

2.7. Cell tracing

Quantitation of *Bcr-Abl* in the nucleus and cytoplasm was carried out by measuring the fluorescence intensity of EGFP, tagged to the *Bcr-Abl*, as previously described [18]. All the images were analyzed using analySIS® software (Soft Imaging System, Lakewood, CO).

2.8. Statistical analysis

All experiments were done at least in triplicate ($n \geq 3$). The difference between the percent nuclear intensity values (for Fig. 4)

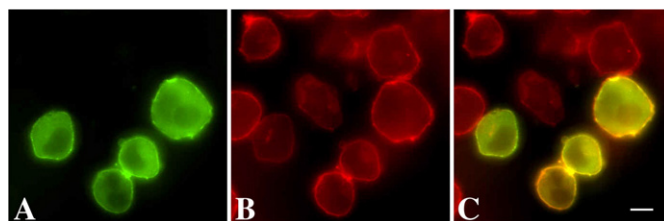


Fig. 1. EGFP-*Bcr-Abl* localization in K562 cells. A. localization of *Bcr-Abl* via EGFP. B. Actin staining of cells. C. Overlay of EGFP-*Bcr-Abl* localization with actin. White scale bar, 5 μ m.

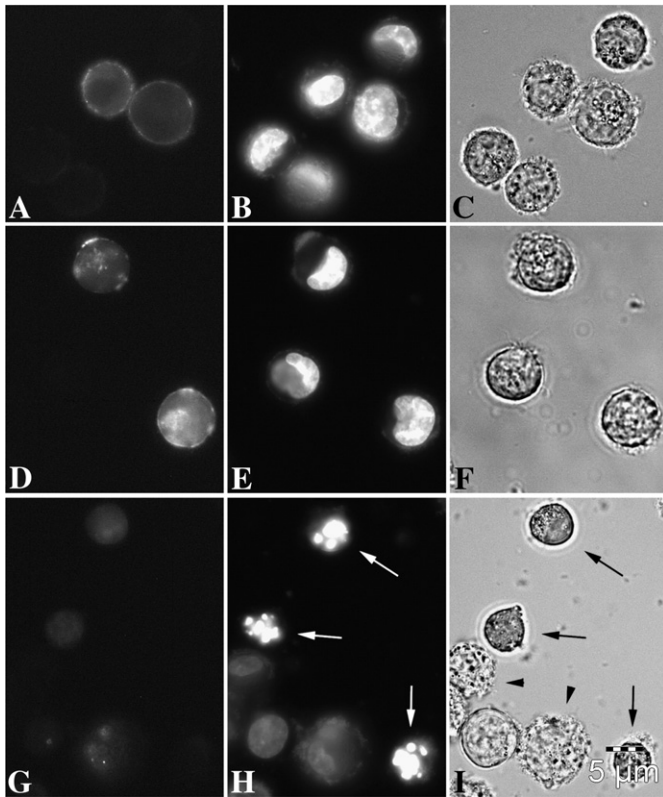


Fig. 2. A–C. EGFP-*Bcr-Abl* transfected into K562 cells; fluorescent (EGFP), nuclear staining with H33342, and phase contrast images, respectively. D–F. EGFP-1NLS-*Bcr-Abl* transfected into K562 cells; fluorescent (EGFP), nuclear staining with H33342, and phase contrast images, respectively. G–I. EGFP-4NLS-*Bcr-Abl* transfected into K562 cells; fluorescent (EGFP), nuclear staining with H33342, and phase contrast images, respectively. White arrows (H) indicate apoptotic cells undergoing massive DNA segmentation. Black arrows (I) indicate that these same cells have undergone cell shrinkage, a morphological hallmark of apoptosis [20–24]. Black arrowheads (I) show cells undergoing zeiotic/cytoplasmic blebbing. Scale bar (5 μm) representative for all panels (A–I).

was analyzed using an unpaired *t*-test with Welch's correction. One-way ANOVA with Tukey's multiple comparisons post-test was used to assess the differences between relative fluorescence intensity values from the caspase-3 assay (Fig. 5). All statistics were calculated using GraphPad Prism (San Diego, CA).

3. Results

When transfected into K562 cells, *Bcr-Abl* (pEGFP-*Bcr-Abl*) localizes in the cytoplasm and forms a distinctive ring around the cell (Fig. 1). This localization is indicative of binding to actin, and is expected due to previous reports of *Bcr-Abl* localization with actin [19]. Co-localization of EGFP-*Bcr-Abl* and actin is shown in Fig. 1.

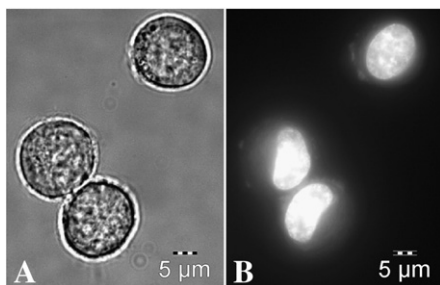


Fig. 3. Healthy K562 cells. Left panel, phase contrast image. Right panel, nuclear staining with H33342. Nuclei of healthy cells are either round/oval or "kidney" shaped.

Table 1

DNA segmentation in K562 cells transfected with EGFP-*Bcr-Abl*, EGFP-1NLS-*Bcr-Abl*, or EGFP-4NLS-*Bcr-Abl*.

Construct transfected	No. of cells transfected	No. transfected cells with segmented DNA	Percentage of cells with segmented DNA
EGFP- <i>Bcr-Abl</i>	178	7	3.9
EGFP-1NLS- <i>Bcr-Abl</i>	154	5	3.2
EGFP-4NLS- <i>Bcr-Abl</i>	375	46	12.3

Additional nuclear localization signal(s) were added to EGFP-*Bcr-Abl* to attempt to overcome *Bcr-Abl* binding to actin. Two plasmids were created, one with 1 NLS subcloned to EGFP-*Bcr-Abl*, and one with 4 NLSs subcloned to EGFP-*Bcr-Abl*. When transfected into K562 cells, only EGFP-4NLS-*Bcr-Abl* localized to the nucleus (Fig. 2G) with the distinct absence of the actin ring surrounding the cell (compared to 2A, wt-*Bcr-Abl*). The 1NLS construct, while somewhat dispersed throughout the cell, still formed a peripheral actin ring (Fig. 2D), just like wt-*Bcr-Abl* (Figs. 2A and 1).

Next, cell studies demonstrating apoptosis were performed on *Bcr-Abl*, 4NLS-*Bcr-Abl*, and 1NLS-*Bcr-Abl*. For comparison, Fig. 3 shows healthy K562 cells. Phase contrast images show round, healthy cells (Fig. 3, left panel), while H33342 staining indicates normal (unsegmented) nuclei (Fig. 3, right panel). Nuclei in healthy K562 cells are round/oval or "kidney" shaped (Fig. 3, right panel).

Twenty-four hours after transfection, cytochemical analyses of apoptosis, including overall cell morphology (Fig. 2C,F, and I) and DNA morphology/segmentation (Fig. 2B,E, and H), were examined.

Morphological changes indicating apoptosis include zeiotic and cytoplasmic blebbing, cell shrinkage, and fragmentation of cells into smaller bodies [20–24]. These morphological changes are seen obviously in cells transfected with 4NLS-*Bcr-Abl*, comparing Fig. 2I (apoptosis) to Fig. 2C and F (no apoptosis). Black arrows indicate shrunken cells (with cell shrinkage indicating apoptosis). Black arrowheads (2I) show cells undergoing zeiotic/cytoplasmic blebbing.

The characteristic change in nuclear morphology (DNA segmentation) is "the most accurate indicator of the involvement of apoptosis in the death of a cell" [22], where the nucleus changes shape from the normal round/oval shape into smaller, non-homogeneous segments. As shown in Fig. 2H, cells transfected with 4NLS-*Bcr-Abl* show this characteristic DNA segmentation into smaller pieces (white arrows), not seen in other cells (compare to Fig. 2B and E), including healthy cells (Fig. 3, right panel).

Transfected cells were also counted for DNA segmentation or nuclear morphology changes, an accurate indicator of apoptosis [22]. As shown in Table 1, cells transfected with EGFP-4NLS-*Bcr-Abl* had a higher percentage of cells with apoptotic nuclei than EGFP-1NLS-*Bcr-Abl* and EGFP-*Bcr-Abl*. Only cells with obvious DNA segmentation (more than two nuclear fragments formed) were counted as segmented.

Bcr-Abl is known to form homodimers (tetramers) [25,26]. To determine if the 4NLS-*Bcr-Abl* was capable of multimerizing with *Bcr-Abl*, and altering its localization, a co-transfection (co-localization) experiment was performed. EGFP-4NLS-*Bcr-Abl* with mutated EGFP chromophore (not fluorescent) was transfected with fluorescent EGFP-*Bcr-Abl*. If the 4NLS-*Bcr-Abl* protein is able to drag *Bcr-Abl* into

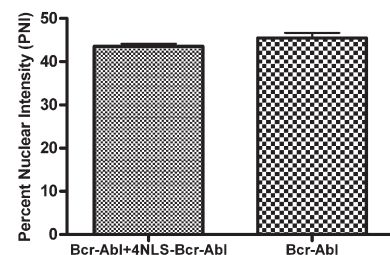


Fig. 4. Percent nuclear intensity for cells transfected with EGFP-*Bcr-Abl* alone (right column) or EGFP-*Bcr-Abl* and 4NLS-*Bcr-Abl* (left column). *n* = 5 cells for each group.

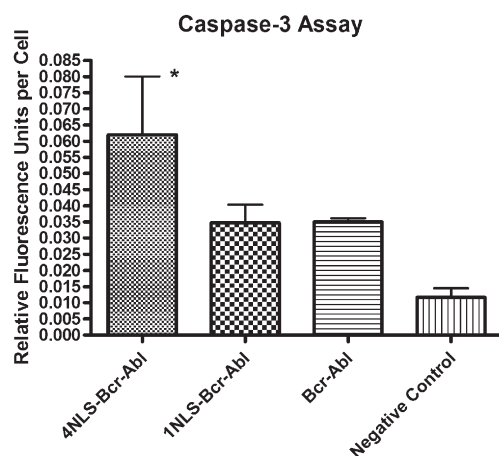


Fig. 5. Caspase-3 activity in K562 cells transfected with EGFP-4NLS-*Bcr-Abl*, EGFP-1NLS-*Bcr-Abl*, EGFP-*Bcr-Abl*, or pGL3basic plasmid (a negative control; plasmid is promoter- and enhancer-less and therefore nothing is expressed). * $p < 0.05$; $n = 3$. Statistical significance determined using one-way Anova with Tukey's correction.

the nucleus, EGFP fluorescence will be detected in the nucleus. If 4NLS-*Bcr-Abl* does not drag *Bcr-Abl* into the nucleus, EGFP-*Bcr-Abl* will remain in the cytoplasm. For this analysis, a semi-quantitative assay was used that measured the fluorescence intensity in the nucleus in the co-transfected cells vs. the singly transfected (with EGFP-*Bcr-Abl*) cells, normalized to each cell's cytoplasmic intensity. These nuclear to cytoplasmic intensities were termed "percent nuclear intensity." 4NLS-*Bcr-Abl* did not "capture" wt-*Bcr-Abl* and drag it into the nucleus, since the nuclear intensity of wt-EGFP-*Bcr-Abl* did not change in the presence of the 4NLS-*Bcr-Abl* construct (Fig. 4). This result is not unexpected since the presence of strong NLSs would presumably drive any protein it was attached to immediately into the nucleus. From this result, it was determined that cytoplasmic depletion of *Bcr-Abl* by 4NLS-*Bcr-Abl* was not occurring.

Next, the caspase-3 assay was used to determine mid-stage apoptosis. Caspases, from cysteine-aspartate proteases, are a group of proteolytic enzymes that perpetuate the apoptotic signal by cleavage of proteins such as actin, lamins, fodrin, ICAD, and PARP. Prior to receiving the apoptotic signal, caspases are present in cells in an inactive pro-enzyme form. The caspase cascade starts with the activation of the initiator caspases (caspase-2, -8, -9, and -10), which then activate effector caspases (caspase-3, -6, and -7). Both caspase-3 and caspase-7 cleave the peptide sequence DEVD, which makes it an ideal substrate for use in measuring apoptosis as a majority of the apoptotic signaling pathways converge on these effector caspases. The caspase-3 assay used measures the cleavage of a substrate with the amino acid sequence DEVD. Caspase-3 activity (Fig. 5) was determined in several treatment groups, including EGFP-4NLS-*Bcr-Abl*, EGFP-1NLS-*Bcr-Abl*, EGFP-*Bcr-Abl*, or a negative control (transfected with pGL3 basic plasmid which has no promoter or enhancer and hence is not expressed). As shown in Fig. 5, only cells transfected with EGFP-4NLS-*Bcr-Abl* showed a statistically significant increase in the caspase activity compared to the negative control.

4. Discussion/Conclusions

Nuclear localization of *Bcr-Abl* converts it from an oncogene to an apoptotic factor. The nuclear localization could not be achieved without adding multiple NLSs to *Bcr-Abl*. Once additional NLSs were added to *Bcr-Abl*, this caused apoptosis of CML cells (K562 cells) measured by morphologic changes (cytoplasmic blebbing and cell shrinkage), DNA segmentation (nuclear morphology changes), and the caspase-3 assay. This critical finding shows that the change in the location of *Bcr-Abl* from cytoplasmic to nuclear dramatically alters its function.

Nuclear entrapment and cytoplasmic depletion of wt-*Bcr-Abl* may have a synergistic effect on cell death. The nuclear entrapment results in apoptosis via the *Abl* domain which can cause cell death by stabilizing p73 and activating its pro-apoptotic functions [2,27,28]. Cytoplasmic depletion of wt-*Bcr-Abl* will remove its ability to interact with the signal transduction proteins involved in gene transcription, mitochondrial processing of apoptotic responses, cytoskeletal organization, and degradation of inhibitory proteins [29]. Here we report that ectopically expressed *Bcr-Abl* directed to the nucleus is sufficient to induce apoptosis without cytoplasmic depletion. However, it may be speculated that coupling cytoplasmic depletion with nuclear entrapment will synergistically enhance the apoptotic signal. To this end, our ultimate goal is to deplete wt-*Bcr-Abl* from the cytoplasm, and direct it to the nucleus by our previously described "protein switch" technology [18,30]. We exploit known dimerization domains (DD) of proteins to capture them and move them to a different subcellular compartment. An ectopically expressed "protein switch" can be designed to target any protein with a DD. The protein switch also contains inducible signal sequences to localize to a starting compartment in the cell (e.g., cytoplasm). Upon addition of ligand, the protein switch can move to a different subcellular compartment (e.g., nucleus). Our ultimate goal is to use the protein switch [18,30] to control the subcellular location of *Bcr-Abl*, and convert *Bcr-Abl* from an oncogene to an apoptotic factor.

Alternative therapies for CML are needed, despite the "blockbuster" results with Gleevec. Gleevec is not a cure for CML, and patients need to take it for the rest of their lives. Gleevec is also known to have severe side effects including cardiotoxicity [11] and the possibility of developing other cancers (due to blockade of tumor suppressor p63) [12]. Importantly, Gleevec resistance mostly occurs due to different point mutations in *Bcr-Abl* that make traditional small molecule inhibitors (like Gleevec) unable to bind/inhibit *Bcr-Abl*. In some cases, a decrease in Gleevec bioavailability/cell exposure and upregulation of drug efflux pumps [6,10] have led to resistance.

The protein switch concept is also being tested in our laboratory with the anti-apoptotic factor survivin, and the tumor suppressor p53 (mislocalized in cancers). Changing localization to alter function may prove to be a new therapeutic strategy for many types of cancer, including CML [31].

Acknowledgements

Funding was provided by NIH R01 CA129528. We acknowledge the use of DNA/Peptide Core supported by the NCI Cancer Center Support Grant P30 CA042014 awarded to Huntsman Cancer Institute. We would like to thank David W. Woessner for technical assistance. We also thank S.W. Kim, K. Elenitoba-Johnson, J. Yockman, T. Cheatham, J. R. Davis, M. Mossalam, and other lab members.

References

- [1] J.D. Rowley, Letter: a new consistent chromosomal abnormality in chronic myelogenous leukaemia identified by quinacrine fluorescence and Giemsa staining, *Nature*. 243 (5405) (1973) 290–293.
- [2] P. Vigneri, J.Y. Wang, Induction of apoptosis in chronic myelogenous leukemia cells through nuclear entrapment of *BCR-ABL* tyrosine kinase, *Nat. Med.* 7 (2) (2001) 228–234.
- [3] B.J. Druker, S. Tamura, E. Buchdunger, S. Ohno, G.M. Segal, S. Fanning, J. Zimmermann, N.B. Lydon, Effects of a selective inhibitor of the *Abl* tyrosine kinase on the growth of *Bcr-Abl* positive cells, *Nat. Med.* 2 (5) (1996) 561–566.
- [4] R. Oldham, R. Dillman, Gold standard or wrong standard? *Cancer Biother. Radiopharm.* 19 (3) (2004) 271–272.
- [5] K. Peggs, Imatinib mesylate—gold standards and silver linings, *Clin. Exp. Med.* 4 (1) (2004) 1–9.
- [6] M. Baccarani, G. Saglio, J. Goldman, A. Hochhaus, B. Simonsson, F. Appelbaum, J. Apperley, F. Cervantes, J. Cortes, M. Deininger, A. Gratwohl, F. Guilhot, M. Horowitz, T. Hughes, H. Kantarjian, R. Larson, D. Niederwieser, R. Silver, R. Hehlmann, Evolving concepts in the management of chronic myeloid leukemia. Recommendations from an expert panel on behalf of the European Leukemianet, *Blood* 108 (6) (2006) 1809–1820.

- [7] M.E. Gorre, M. Mohammed, K. Ellwood, N. Hsu, R. Paquette, P.N. Rao, C.L. Sawyers, Clinical resistance to STI-571 cancer therapy caused by *BCR-ABL* gene mutation or amplification, *Science* 293 (5531) (2001) 876–880.
- [8] N.P. Shah, C.L. Sawyers, Mechanisms of resistance to STI571 in Philadelphia chromosome-associated leukemias, *Oncogene* 22 (47) (2003) 7389–7395.
- [9] S. Roumiantsev, N.P. Shah, M.E. Gorre, J. Nicoll, B.B. Brasher, C.L. Sawyers, R.A. Van Etten, Clinical resistance to the kinase inhibitor STI-571 in chronic myeloid leukemia by mutation of Tyr-253 in the *Abl* kinase domain P-loop, *Proc. Natl. Acad. Sci. U.S.A.* 99 (16) (2002) 10700–10705.
- [10] J.V. Melo, T.P. Hughes, J.F. Apperley, Chronic myeloid leukemia, *Hematology (Am Soc Hematol Educ Program)* (2003) 132–152.
- [11] R. Kerkela, L. Grazette, R. Yacobi, C. Iliescu, R. Patten, C. Beahm, B. Walters, S. Shevtsov, S. Pesant, F.J. Clubb, A. Rosenzweig, R.N. Salomon, R.A. Van Etten, J. Alroy, J.B. Durand, T. Force, Cardiotoxicity of the cancer therapeutic agent imatinib mesylate, *Nat. Med.* 12 (8) (2006) 908–916.
- [12] W.M. Ongkeko, Y. An, T.S. Chu, J. Aguilera, C.L. Dang, J. Wang-Rodriguez, Gleevec suppresses p63 expression in head and neck squamous cell carcinoma despite p63 activation by DNA-damaging agents, *Laryngoscope* 116 (8) (2006) 1390–1396.
- [13] H. Francois, P. Coppo, J.P. Hayman, B. Fouqueray, B. Mougenot, P. Ronco, Partial fanconi syndrome induced by imatinib therapy: a novel cause of urinary phosphate loss, *Am. J. Kidney Dis.* 51 (2) (2008) 298–301.
- [14] B. Calabretta, D. Perrotti, The biology of CML blast crisis, *Blood* 103 (11) (2004) 4010–4022.
- [15] J.M. Goldman, J.V. Melo, Chronic myeloid leukemia—advances in biology and new approaches to treatment, *N. Engl. J. Med.* 349 (15) (2003) 1451–1464.
- [16] C.W. Cody, D.C. Prasher, W.M. Westler, F.G. Prendergast, W.W. Ward, Chemical structure of the hexapeptide chromophore of the *Aequorea* green-fluorescent protein, *Biochemistry* 32 (5) (1993) 1212–1218.
- [17] M. Ormo, A.B. Cubitt, K. Kallio, L.A. Gross, R.Y. Tsien, S.J. Remington, Crystal structure of the *Aequorea victoria* green fluorescent protein, *Science* 273 (5280) (1996) 1392–1395.
- [18] M. Kakar, J.R. Davis, S.E. Kern, C.S. Lim, Optimizing the protein switch: altering nuclear import and export signals, and ligand binding domain, *J. Control. Release* 120 (3) (2007) 220–232.
- [19] O. Hantschel, S. Wiesner, T. Guttler, C.D. Mackereth, L.L. Rix, Z. Mikes, J. Dehne, D. Gorlich, M. Sattler, G. Superti-Furga, Structural basis for the cytoskeletal association of *Bcr-Abl/c-Abl*, *Mol. Cell.* 19 (4) (2005) 461–473.
- [20] R.A. Schwartzman, J.A. Cidlowski, Apoptosis: the biochemistry and molecular biology of programmed cell death, *Endocr. Rev.* 14 (2) (1993) 133–151.
- [21] I. Vermes, C. Haanen, Apoptosis and programmed cell death in health and disease, *Adv. Clin. Chem.* 31 (1994) 177–246.
- [22] M.C. Willingham, Cytochemical methods for the detection of apoptosis, *J. Histochem. Cytochem.* 47 (9) (1999) 1101–1110.
- [23] C.D. Bortner, J.A. Cidlowski, Apoptotic volume decrease and the incredible shrinking cell, *Cell Death Differ.* 9 (12) (2002) 1307–1310.
- [24] C.D. Bortner, J.A. Cidlowski, Uncoupling cell shrinkage from apoptosis reveals that Na⁺ influx is required for volume loss during programmed cell death, *J. Biol. Chem.* 278 (40) (2003) 39176–39184.
- [25] X. Zhao, S. Ghaffari, H. Lodish, V.N. Malashkevich, P.S. Kim, Structure of the *Bcr-Abl* oncoprotein oligomerization domain, *Nat. Struct. Biol.* 9 (2) (2002) 117–120.
- [26] J.R. McWhirter, D.L. Galasso, J.Y. Wang, A coiled-coil oligomerization domain of *Bcr* is essential for the transforming function of *Bcr-Abl* oncoproteins, *Mol. Cell. Biol.* 13 (12) (1993) 7587–7595.
- [27] A. Aloisi, S. Di Gregorio, F. Stagno, P. Guglielmo, F. Mannino, M.P. Sormani, P. Bruzzi, C. Gambacorti-Passerini, G. Saglio, S. Venuta, R. Giustolisi, A. Messina, P. Vigneri, *BCR-ABL* nuclear entrapment kills human CML cells: ex vivo study on 35 patients with the combination of imatinib mesylate and leptomycin B, *Blood* 107 (4) (2006) 1591–1598.
- [28] J.Y. Wang, Regulation of cell death by the *Abl* tyrosine kinase, *Oncogene* 19 (49) (2000) 5643–5650.
- [29] Z. Dai, P. Kerzic, W.G. Schroeder, I.K. McNiece, Deletion of the Src homology 3 domain and C-terminal proline-rich sequences in *Bcr-Abl* prevents *Abl* interactor 2 degradation and spontaneous cell migration and impairs leukemogenesis, *J. Biol. Chem.* 276 (31) (2001) 28954–28960.
- [30] M. Kakar, A.B. Cadwallader, J.R. Davis, C.S. Lim, Signal sequences for targeting of gene therapy products to subcellular compartments: the role of CRM1 in nucleocytoplasmic shuttling of the protein switch, *Pharm. Res.* 24 (11) (2007) 2146–2155.
- [31] J.R. Davis, M. Kakar, C.S. Lim, Controlling protein compartmentalization to overcome disease, *Pharm. Res.* 24 (1) (2007) 17–27.